Overite, segelerite, and jahnsite: a study in combinatorial polymorphism

PAUL B. MOORE AND TAKAHARU ARAKI

Department of the Geophysical Sciences
The University of Chicago
Chicago, Illinois 60637

Abstract

Overite, $[Mg(H_2O)_4]_2[Ca_2Al_2(OH)_2(PO_4)_4]$, $Z = 4$, $a = 14.723(14)$, $b = 18.746(16)$, $c = 7.107(4)$A, orthorhombic, space group *Pbca*; and segelerite, $[Mg(H_2O)_4]_2$ $[Ca_2Fe_2^{3+}(OH)_2(PO_4)_4]$, $Z = 4$, $a = 14.826(5)$, $b = 18.751(4)$, $c = 7.307(1)$A, orthorhombic, space group *Pbca*, are related in a combinatorial way to jahnsite, $[Mg(H_2O)_4]_2$ $[CaMn^{2+}Fe_2^{3+}(OH)_2(PO_4)_4]$, $Z = 2$, $a = 14.94(2)$, $b = 7.14(1)$, $c = 9.93(1)$A, $\beta = 110.16(8)°$, monoclinic, space group *P2/a*. $R = 0.090$ for 1915 reflections (overite) and 0.236 for 2387 reflections (segelerite).

Overite, segelerite, and jahnsite are based on dense slabs of composition $[X_2^{2+}M_2^{3+}(OH)_2(PO_4)_4]$ whose maximal symmetry is *Bmam*. Linkages to the slabs by $[Mg(O_P)_2(H_2O)_4]$ octahedra determine the discrete kinds of isomerism. In overite and segelerite, the arrangement is *trans*-$[Mg(O_P)_2(H_2O)_4]$ and in jahnsite it is alternately *cis*-$[Mg(O_P)_2(H_2O)_4]$ and *trans*-$[Mg(O_P)_2(H_2O)_4]$, where O_P is a phosphate oxygen.

Overite, which is well-refined, has average distances [6]Ca–O 2.40, [6]Al–O 1.91, [6]Mg–O 2.08, [4]P(1)–O 1.54, and [4]P(2)–O 1.54A. A herring-bone pattern of hydrogen bonds is arranged normal to the [010] direction.

Introduction

Overite, segelerite, and jahnsite belong to a large family of structures which are derived from octahedral corner-sharing chains (Moore 1970, 1975). The family consists of low-temperature minerals, difficult to distinguish by casual inspection. Even their powder patterns closely resemble each other. Overite and segelerite belong to the same structure type, and jahnsite is closely related (Moore, 1974; Moore and Araki, 1974). Evidence in these earlier studies suggested that, although the compositions are based on $M^{2+}(H_2O)_4[X^{2+}M^{3+}(OH)(PO_4)_2]$, where $M^{2+} = Mg^{2+},Mn^{2+}$; $X^{2+} = Ca^{2+},Mn^{2+},Fe^{2+}$; and $M^{3+} = Fe^{3+},Al^{3+}$, and thus segelerite and jahnsite are sensibly dimorphic, subtle structural differences exist. Moore and Araki (1974) suggested that the differences were based on discrete isomerisms of ligands about the $M^{2+}(O_P)_2(H_2O)_4$ octahedra, where $O_P = $ phosphate oxygen.

Combinatorial isomerism is one of the underlying principles which govern the great species diversity among low-temperature oxysalts. It was desirable, therefore, in light of the jahnsite structure, to extend our inquiry to the closely-related segelerite and to explore the differing regions in the two structures. A structural principle which governs diversity of species is most desirable. Not only are the relationships between structure types made more evident, but the opportunity also exists for generating further as yet unknown structures, and to place their classification on the firm ground of systematic graphical enumeration where all the possible structures, both real and hypothetical, are countable.

Experimental procedure

The details of the experimental section are summarized in Table 1. Cell parameters for overite were determined on calibrated precession photographs, and those for segelerite are quoted from Moore (1974). Specific gravity determinations are quoted from Larsen (1940) and Moore (1974) for overite and segelerite respectively. The overite crystal, U.S. National Museum R7898 (type), was kindly donated by Mr. John S. White, Jr., of that institution. For the segelerite, we selected a crystal from the type specimen.

Precession photographs of both overite and segele-

Table 1. Overite and segelerite. Experimental details

(A) Crystal Cell Data

	OVERITE	SEGELERITE
$a(\text{Å})$	14.723(14)	14.826(5)
$b(\text{Å})$	18.746(16)	18.751(4)
$c(\text{Å})$	7.107(4)	7.307(1)
Space group	Pbca	Pbca
Z	8	8
Formula	$CaMg(H_2O)_4Al(OH)(PO_4)_2$	$CaMg(H_2O)_4Fe^{3+}(OH)(PO_4)_2$
$\rho(\text{calc, gm cm}^{-3})$	2.51	2.61
Specific gravity	2.53	2.67
$\mu(\text{cm}^{-1})$	11.8	30.7

(B) Intensity Measurements

Diffractometer	Pailred	Picker Four-circle
Crystal size (mm)	0.30(||a), 0.25(||b), 0.25(||c)	0.10(||a), 0.10(||b), 0.30(||c)
Maximum $\sin\theta/\lambda$	0.75	0.71
Crystal orientation	c-axis rotation	ϕ-axis ||c
Scan speed	$1° \text{ min}^{-1}$	$2° \text{ min}^{-1}$
Base scan width	2.4° to 5.2°	2.3°
Background counts	Stationary, 20 sec at beginning and end of scan	
Radiation	MoK_{α_1} ($\lambda = 0.70926\text{Å}$), graphite monochromator	
Independent F_O	3392	3628

(C) Refinement of the Structures

R-indices		F_O	Number	R	R_W		F_O	Number	R	R_W
	Above	0.0	3392	0.142	0.081	Above	0.0	3628	0.281	0.172
	"	10.0	1915	0.090	0.060	"	12.5	2387	0.236	0.167
	"	30.0	754	0.046	0.051	"	37.5	850	0.110	0.119
c_O		$3.7(3) \times 10^{-7}$					not applied			
Goodness-of-fit		3.54					4.00			

rite suggested that the structure analysis would not be a simple procedure, owing to the prevalence of weak to unobservable reflections: over 80 percent estimated to fall within this range. The substructure reflections suggest space group *Bmam,* as proposed by Larsen (1940). Moore (1974) proposed space group *Pcca,* the weak superstructure reflections violating the space group proposed by Larsen.

At first, structure analysis was inaugurated on segelerite and the general features of the substructure were revealed upon subsequent Patterson synthesis. It was apparent that deviations leading to the primi-tive space group were determined by Mg^{2+} and its oxygen environment. Using the structure of jahnsite as a guide (Moore and Araki, 1974), some progress was made. Unfortunately, the water molecules coordinated to Mg^{2+} were split, suggesting disorder. Long-exposure precession photographs about the three principal zones revealed that the space group *Pcca* was violated by extremely weak reflections (F_o < 12, see Table 4), but that *Pbca* was consistent with systematic absences on these photographs. The space group *Pbca* required a new choice of asymmetric unit, and the ensuing analysis afforded a uniform

environment of spherical contours for oxygens about Mg. A γ'-synthesis (Ramachandran and Srinivasan, 1970) revealed all non-hydrogen atoms, and least-squares refinement was initiated. Despite the plausibility of the structure, including satisfactory bond distances, the reliability index would not converge below $R = 0.28$ for all 3628 reflections. We concluded that the structure was formally correct but that the data were of inferior quality owing to the prevalence of very weak reflections.

We then decided to perform the same investigation on the overite isotype, since large (up to 1 mm) crystals could be obtained and since the water molecules and Mg atoms would play a more significant role in the structure factors, owing to the presence of lighter Al in place of Fe. Indeed, the trial parameters obtained from segelerite converged smoothly to $R = 0.14$ for all 3392 reflections gathered from overite.

Owing to the low absorption coefficient, μ, for overite and the small size of the segelerite crystal, no correction for absorption anisotropy was applied in both crystals. Symmetry-equivalent reflections were averaged and $I_o < 2\sigma(I_o)$ was set $I_o = \sigma(I_o)$. Full-matrix least-squares refinement proceeded from FLMXLS, a program with options for bond distances and angles developed by T. Araki, whose roots are found in the familiar ORFLS programs of Busing *et al.* (1962). For refinement, we employed Ca^{2+}, Mg^{2+}, Al^{3+}, Fe^{3+}, P^0, and O^{1-} scattering factors obtained from the tables of Cromer and Mann (1968). Anomalous dispersion correction for Ca, Mg, Al, Fe, and P employed the tables of Cromer and Liberman (1970). The weighted reliability index, R_w, equals $\{[\Sigma_w(|F_o| - |F_c|)^2]/\Sigma_w F_o^2\}^{1/2}$, with $w = \sigma^{-2}(F_o)$ and the refinements minimized $\Sigma_w(F_o - F_c)^2$. The secondary extinction coefficient c_o, was refined for overite (Zachariasen, 1968). The goodness-of-fit, $\Sigma_w(F_o - F_c)^2/\Sigma(n - m)$, where n = number of independent data and m = number of parameters, is listed in Table 1 along with the other convergences.

The results in Table 1 suggest that the presence of strongly scattering Fe^{3+} in segelerite, indeed, "masked" the weak contributions by H_2O and Mg in the structure. Since a large crystal of overite was used, it was possible to recover most of the contributions by the weak scatterers which contributed primarily to the superstructure reflections.

Atomic coordinate parameters and isotropic thermal vibration parameters are presented in Table 2. Bond distances and angles for overite are listed in Table 3; owing to the inferior quality of the data, only bond distances are listed for segelerite. Table 4 lists the structure factors for overite and segelerite.[1]

Segelerite and jahnsite: examples of combinatorial polymorphism

To most clearly grasp the interesting implications

Table 2. Overite and segelerite. Atomic coordinates and isotropic thermal vibration parameters

	OVERITE					SEGELERITE			
Atom	x	y	z	B(Å²)	Atom	x	y	z	B(Å²)
Ca	0.00588(8)	0.24948(8)	0.2424(2)	1.30(2)	Ca	0.0086(2)	0.2469(2)	0.2442(5)	1.33(4)
Mg	0.12809(13)	0.50033(11)	0.7518(3)	1.07(2)	Mg	0.1264(3)	0.5009(3)	0.7522(9)	1.14(6)
Al	0.25686(11)	0.25054(10)	0.2490(2)	0.65(2)	Fe	0.2593(1)	0.2486(1)	0.2421(4)	0.64(3)
P(1)	0.38899(9)	0.34886(7)	0.4936(2)	0.72(2)	P(1)	0.3967(2)	0.3497(2)	0.4914(6)	0.79(4)
O(1)	0.3431(3)	0.3192(2)	0.6707(6)	1.30(6)	O(1)	0.3497(6)	0.3212(5)	0.6658(16)	1.25(16)
O(2)	0.3566(2)	0.3074(2)	0.3177(5)	0.84(5)	O(2)	0.3668(6)	0.3076(5)	0.3217(14)	0.76(13)
O(3)	0.4920(3)	0.3318(2)	0.5104(6)	1.16(6)	O(3)	0.4992(5)	0.3326(5)	0.5037(19)	1.28(14)
O(4)	0.3738(3)	0.4285(2)	0.4766(6)	1.25(6)	O(4)	0.3821(6)	0.4281(5)	0.4869(17)	1.22(15)
P(2)	0.12512(8)	0.34936(7)	0.5056(2)	0.73(2)	P(2)	0.1225(2)	0.3515(2)	0.5075(6)	0.70(4)
O(5)	0.1551(3)	0.3060(2)	0.6808(6)	1.08(6)	O(5)	0.1536(6)	0.3089(5)	0.6824(15)	1.11(15)
O(6)	0.1713(3)	0.3224(2)	0.3254(6)	1.20(6)	O(6)	0.1703(7)	0.3255(6)	0.3366(17)	1.63(18)
O(7)	0.0222(3)	0.3312(2)	0.4862(5)	0.91(5)	O(7)	0.0203(6)	0.3300(5)	0.4905(19)	1.32(15)
O(8)	0.1390(3)	0.4289(2)	0.5304(6)	1.04(5)	O(8)	0.1400(5)	0.4314(5)	0.5431(13)	0.61(13)
OH	0.2549(3)	0.2912(2)	-.0004(5)	0.84(5)	OH	0.2577(6)	0.2967(4)	0.0051(19)	1.28(13)
OW(1)	0.2683(3)	0.5080(2)	0.7495(7)	1.41(6)	OW(1)	0.2681(5)	0.5086(5)	0.7551(17)	1.15(14)
OW(2)	-.0129(3)	0.4952(3)	0.7527(8)	1.83(7)	OW(2)	-.0114(7)	0.4913(6)	0.7405(21)	1.83(17)
OW(3)	-.1335(3)	0.4210(2)	0.9591(6)	1.49(6)	OW(3)	0.1325(6)	0.4218(5)	0.9567(15)	0.91(14)
OW(4)	0.1182(3)	0.5792(2)	0.5436(6)	1.46(6)	OW(4)	0.1191(6)	0.5810(6)	0.5504(18)	1.60(18)

Table 3. Overite and segelerite. Polyhedral bond distances and angles†

Al

	O	S
Al -O(2)	1.879(4)	2.03
-O(5)$^{(5)}$	1.898(4)	1.95
-O(1)$^{(5)}$	1.907(5)	1.96
-O(6)	1.923(5)	2.07
-OH	1.930(4)	1.95
-OH$^{(5)}$	1.945(4)	2.10
average	1.914	2.01

	O	S	O–Al–O´ (deg.)
O(1)$^{(5)}$-O(2)	2.601(6)	2.68	86.8(2)
O(6) -O(5)$^{(5)}$	2.629(6)	2.77	86.9(2)
OH -O(5)$^{(5)}$	2.672(5)	2.82	88.5(2)
OH -O(6)	2.687(6)	2.80	88.5(2)
OH$^{(5)}$-O(2)	2.707(5)	2.87	90.1(2)
OH$^{(5)}$-O(5)$^{(5)}$	2.715(6)	2.83	89.9(2)
OH$^{(5)}$-O(1)$^{(5)}$	2.726(6)	2.87	90.1(2)
OH -O(2)	2.729(5)	2.83	91.5(2)
OH -O(1)$^{(5)}$	2.730(6)	2.85	90.7(2)
O(2) -O(6)	2.743(6)	2.94	92.4(2)
OH$^{(5)}$-O(6)	2.753(6)	2.91	90.8(2)
O(5)$^{(5)}$-O(1)$^{(5)}$	2.780(6)	2.92	93.9(2)
average	2.706	2.84	90.0

Ca

	O	S
Ca -O(7)	2.325(4)	2.39
-O(3)$^{(6)}$	2.335(5)	2.37
-O(3)$^{(1)}$	2.377(5)	2.43
-O(7)$^{(5)}$	2.379(4)	2.36
-O(5)$^{(5)}$	2.471(5)	2.43
-O(2)$^{(1)}$	2.487(4)	2.44
average	2.396	2.40
-O(1)$^{(6)}$	*2.790(5)*	*2.76*
-O(6)	*2.855(5)*	*2.89*

Mg

	O	S
Mg -OW(1)	2.069(5)	2.11
- O(8)	2.073(4)	2.02
-OW(2)	2.078(5)	2.05
- O(4)$^{(2)}$	2.082(5)	2.17
-OW(3)	2.095(5)	2.11
-OW(4)	2.096(5)	2.11
average	2.082	2.09

Mg

	O	S	O–Mg–O´ (deg.)
O(4)$^{(2)}$-OW(3)	2.826(7)	2.83	85.2(2)
O(8) -OW(4)	2.836(7)	2.82	85.7(2)
O(8) -OW(1)	2.872(7)	2.85	87.8(2)
O(4)$^{(2)}$-OW(1)	2.898(7)	3.04	88.5(2)
OW(2) -OW(4)	2.901(8)	2.92	88.0(2)
OW(2) -OW(3)	2.955(8)	2.96	90.2(2)
O(4)$^{(2)}$-OW(2)	2.962(7)	3.03	90.8(2)
OW(1) -OW(4)	2.968(8)	2.99	90.9(2)
OW(1) -OW(3)	2.969(8)	2.98	91.0(2)
OW(2) -O(8)	3.007(7)	2.89	92.8(2)
OW(3) -O(8)	5.051(7)	3.03	94.1(2)
O(4)$^{(2)}$-OW(4)	3.083(7)	3.19	95.1(2)
average	2.944	2.96	90.0

P(1)

	O	S
P(1) -O(4)	1.515(4)	1.49
-O(1)	1.532(4)	1.55
-O(2)	1.548(4)	1.53
-O(3)	1.554(4)	1.56
average	1.537	1.53

	O	S	O–P(1)–O´ (deg.)
O(2) -O(3)	2.461(6)	2.42	105.0(2)
O(1) -O(3)	2.481(6)	2.52	107.0(2)
O(1) -O(4)	2.510(6)	2.44	110.9(2)
O(3) -O(4)	2.525(6)	2.50	110.7(2)
O(1) -O(2)	2.527(6)	2.54	110.2(2)
O(2) -O(4)	2.549(6)	2.57	112.7(2)
average	2.509	2.50	109.4

P(2)

	O	S
P(2) -O(8)	1.515(4)	1.54
-O(6)	1.535(4)	1.52
-O(5)	1.551(4)	1.58
-O(7)	1.560(4)	1.57
average	1.540	1.55

	O	S	O–P(2)–O´ (deg.)
O(5) -O(7)	2.443(6)	2.46	103.5(2)
O(6) -O(7)	2.481(6)	2.49	106.6(2)
O(6) -O(8)	2.516(6)	2.53	111.2(2)
O(7) -O(8)	2.532(6)	2.63	110.9(2)
O(5) -O(8)	2.550(6)	2.52	112.6(2)
O(5) -O(6)	2.555(6)	2.56	111.8(2)
average	2.513	2.53	109.4

†Estimated standard errors for overite (O) are stated in parentheses. The bond distances are also listed for segelerite (S). The estimated errors are within ±0.01Å for Me—O and ±0.02Å for O—O´. The equivalent atoms are (1) ½ +x, y, ½ -z; (2) ½ -x, -y, ½ +z; (3) -x, -y, -z; (4) x, -y, ½ +z; (5) x, ½ -y, ½ +z; and (6) ½ +x, ½ -y, -z.

of the crystal structures of the segelerite and jahnsite structure types, it is convenient to express the general formula as $[Mg(H_2O)_4]_2[M_2^{2+}M_2^{3+}(OH)_2(PO_4)_4]$, where $M^{2+} = Ca^{2+}, Mn^{2+}, Fe^{2+}, \ldots$; and $M^{3+} = Fe^{3+}, Al^{3+}$. The structural unit in the first brackets

corresponds to the $Mg(O_P)_2(H_2O)_4$ octahedron, which receives two bonds from phosphate tetrahedra (the O_P oxygens) and four from water molecules. The second brackets include the dense slab whose dimensions are approximately (a,c) of segelerite = (a,b) of

jahnsite = (15.0, 7.0A). In jahnsite the composition of the slab is the same as that of segelerite, except that $M_2^{2+} = Ca^{2+} Mn^{2+}$ in jahnsite, whereas $M_2^{2+} = Ca_2^{2+}$ in segelerite. The difference in cation ordering, however, does not change the symmetry of the slab, which in both structures and in some hypothetical structures has minimal symmetry of an axial *a*-glide plane normal to the *c* axis. The structure-cell parameters are *Z* = 2, *a* = 14.94(2), *b* = 7.14(1), *c* = 9.93(1)A, β = 110.16(8)°, space group *P2/a* for jahnsite, with the slab oriented parallel to the {001} plane.

What is the maximal symmetry for an idealized slab? In asking this question, the space-group genealogy of its derivative structures arising from geometrical distortion is sought. Figure 1 presents a projection of segelerite down *y* within the boundary of a slab, that is, 0 < *y* < ½. Inspection readily shows that the *a* and *c* axes possess pseudo-mirror planes. Translating (0, ¼, 0), we obtain as the maximal group *Bmc'm* (= *Bma'm* = *Bcc'a* = *Bca'a*), the primes denoting the axial direction of finite thickness. Keeping within "same cell" relationships, all derivative
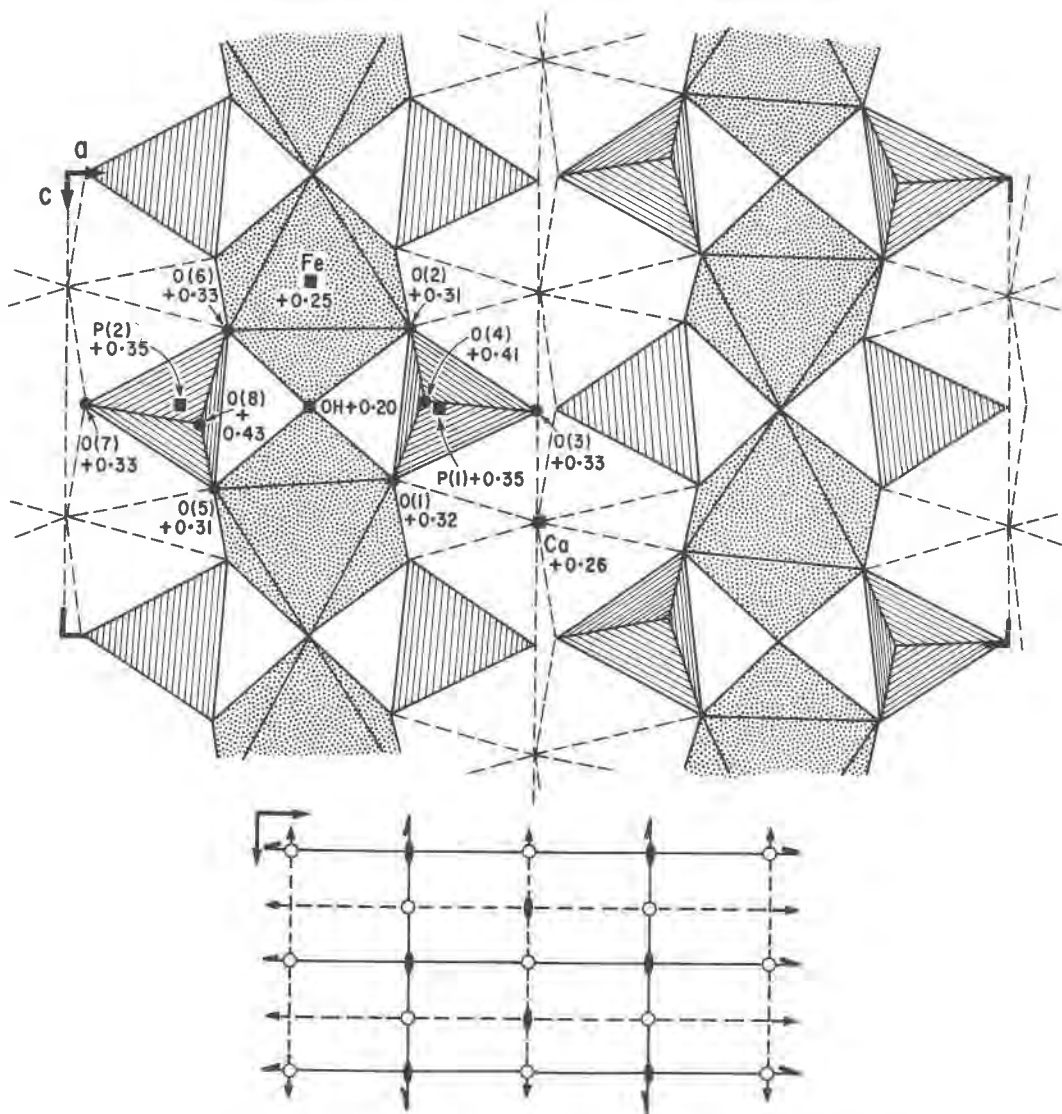

Fig. 1. Structure of segelerite down the [010] axis within 0 < *y* < ½. Atoms designated in the asymmetric unit correspond to Table 2. The Ca–O bonds are dashed in. The symmetry diagram below, drawn half-scale, refers to the supergroup *Bmcm*.

slabs must be subgroups of *Bmc'm*. In Figure 2, the idealized slab is shown down the *z* direction, with the symmetry elements appropriately located. Thirteen symmetry elements can be recognized within the unit slab. The identity, a second inversion center, and the B-centering complete the elements of the space group.

The actual segelerite structure down the *c* axis is featured in Figure 3, but it is more convenient to discuss the structure on the basis of the ideal arrangement in Figure 4a. Regarding the slabs alone, the structure is ideally *Bmam* with $b' = b/2$. This is the subgroup observed by Larsen (1940) for overite. Ordering of the Mg–O octahedra, however, leads to the condition $b' = b$ and the maximal space group *Ibca*. Since the actual structure is based on a nearest subgroup of *Ibca*, that is *Pbca*, local distortions away from the ideal configuration degrade the symmetry. The actual distortion is a combination of twisting of the octahedral chains and distortion of the $Mg(O_P)_2(H_2O)_4$ octahedra, the latter presumably as a result of accommodating unsymmetrical hydrogen bonds. It is noted that all $Mg(O_P)_2(H_2O)_4$ octahedra possess a *trans*-configuration with respect to their ligand environments.

The relationship with jahnsite is immediately obvious, as seen in the ideal arrangement of Figure 4b for the latter compound. Alternate slabs are shifted so that the $Mg(O_P)_2(H_2O)_4$ octahedra possess alternate *cis*- and *trans*-configurations with respect to bonding ligands. Thus, segelerite and jahnsite are combinatorial polymorphs and differ only in the way in which successive slabs are bridged by the insular octahedra. The plane of perfect cleavage in the two structure types is {010} in segelerite (and overite), and {001} in jahnsite, the planes parallel to the dense slabs.

These observations suggest that arrangements in this subfamily of structures are capable of considerable versatility, and challenges for the investigator. Presumably, the twisting of the Me^{3+}–O octahedral chains is related to the sizes of the Me^{2+} cations bonded within the slabs. Thus, a great variety of distortions is possible, all derived from parent space groups of high order. For example, nearest subgroups for segelerite-shaped cells can be those found in *Bmam* and *Ibca*, such as *Pbca*, *Pcca*, *Pcaa*, *Pmam*, etc.

Can an arrangement be found where only *cis*-$Mg(O_P)_2(H_2O)_4$ bridging octahedra occur? One such arrangement is idealized in Figure 4c. It possesses approximate cell dimensions $15 \times 20 \times 7$Å and the
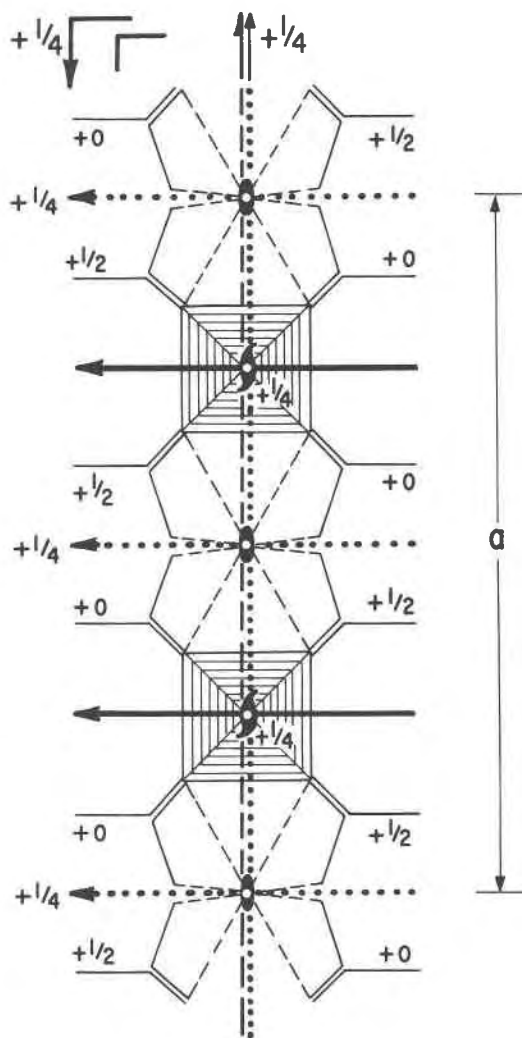

Fig. 2. Idealized slab of octahedra and tetrahedra down the [001] axis showing the loci of the symmetry elements compatible with a slab of *Bmcm*. Note the high symmetry for the idealized slab.

space group *Pbma*. The slabs alone lead to *Cmma*, but steric restrictions limit the ordering scheme for the bridging octahedra. Such a structure will be difficult to test, since it will closely resemble in its crystal-chemical characters the segelerite structure. This emphasizes the fact that members of the jahnsite–segelerite group cannot be easily distinguished through more simple techniques, since their distinguishing character will only be found in the course of detailed single-crystal study. Thus, single-crystal photography is essential in the study of these compounds.

As the slabs are the dominating feature of the structures, it is desirable to express the chemical formulae in such a way that their relationships are ob-
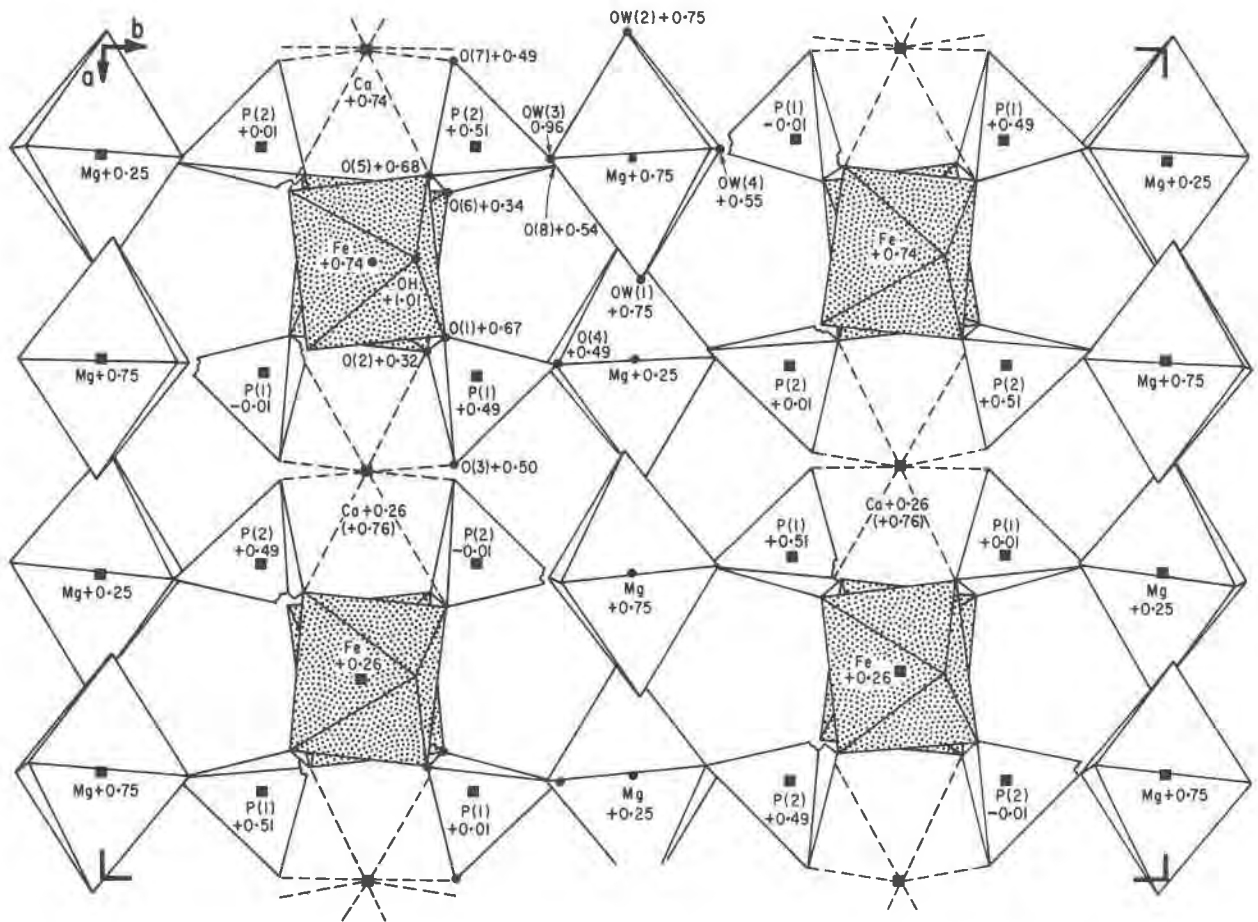
Fig. 3. The real segelerite structure projected down [001]. Note the bridging Mg–O octahedra and the compact $[Ca_2Fe_2^{3+}(OH)_2(PO_4)_4]^{4-}$ slabs. Heights are given as fractional coordinates in z.

vious. We recommend

overite $[Mg(H_2O)_4]_2[Ca_2Al_2(OH)_2(PO_4)_4]$

segelerite $[Mg(H_2O)_4]_2[Ca_2Fe_2^{3+}(OH)_2(PO_4)_4]$

jahnsite $[Mg(H_2O)_4]_2[CaMn^{2+}Fe_2^{3+}(OH)_2(PO_4)_4]$

bearing in mind that *trans*-$[Mg(O_P)_2(H_2O)_4]$ is the configuration for overite and segelerite, and *cis*-$[Mg(O_P)_2(H_2O)_4]$ and *trans*-$[Mg(O_P)_2(H_2O)_4]$ for jahnsite.

Bond distances

Since overite is a well-refined structure, bond distances for that compound will be discussed. The first step is to ascertain hydrogen bonds and then to deter-

mine correlations between deviations in bond strength sums with bond lengths.

Steric restrictions place limits on the loci of hydrogen bonds, the proposed scheme of which is shown in Figure 5. Possible hydrogen atom donors are OH, OW(1), OW(2), OW(3), and OW(4). The proposed scheme is similar to that proposed for jahnsite (Moore and Araki, 1974). The bonds define a herringbone pattern which bridges across the [010] direction. According to this scheme, O(2), O(3), O(5), and O(7) each accepts one hydrogen bond and O(4) and O(8) each receives two bonds. The OH⁻ anion evidently does not form a hydrogen bond, owing to its restricted position: the only possible bond would have to be along an octahedral edge which, owing to
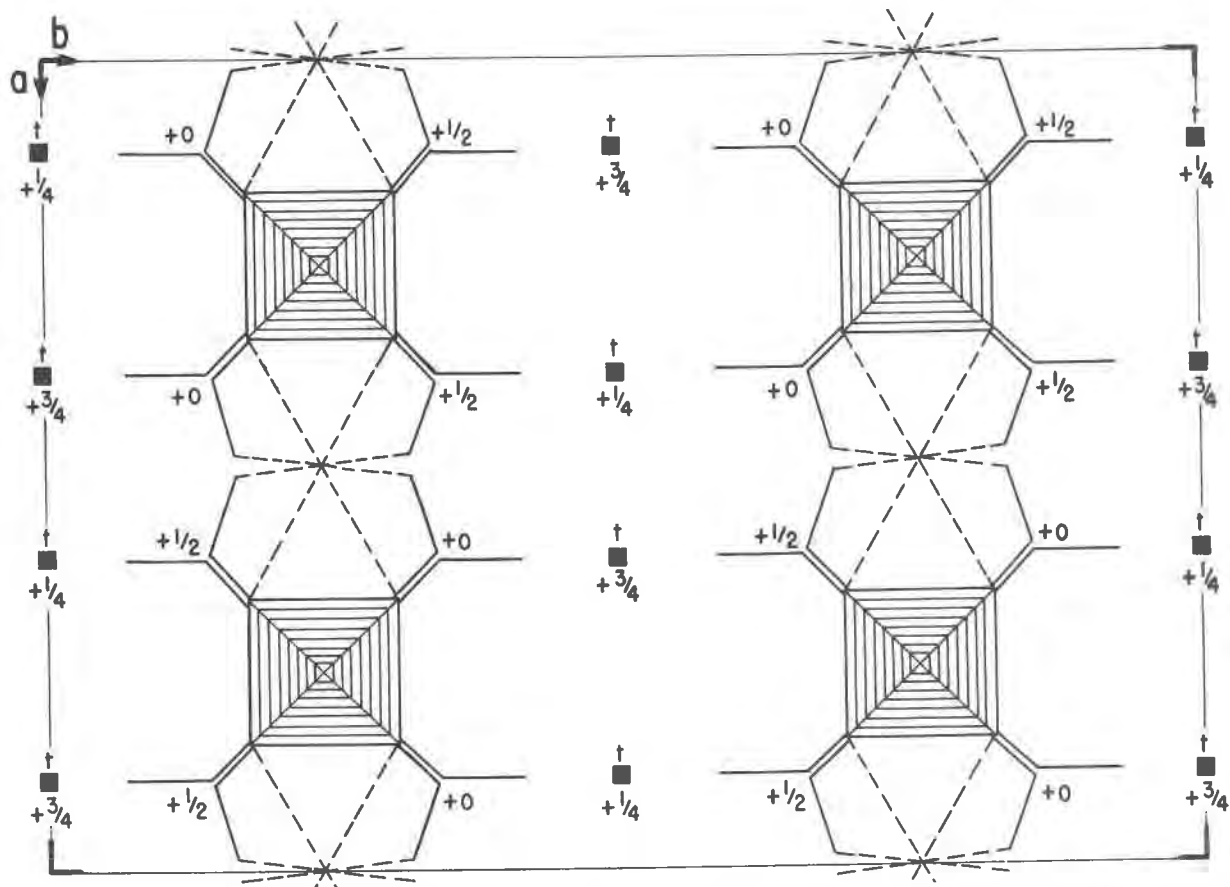
Fig. 4a. Idealized structures of segelerite and overite fully assembled. The solid squares denote the bridging octahedra and "t" denotes *trans*-configuration of ligands about these octahedra.
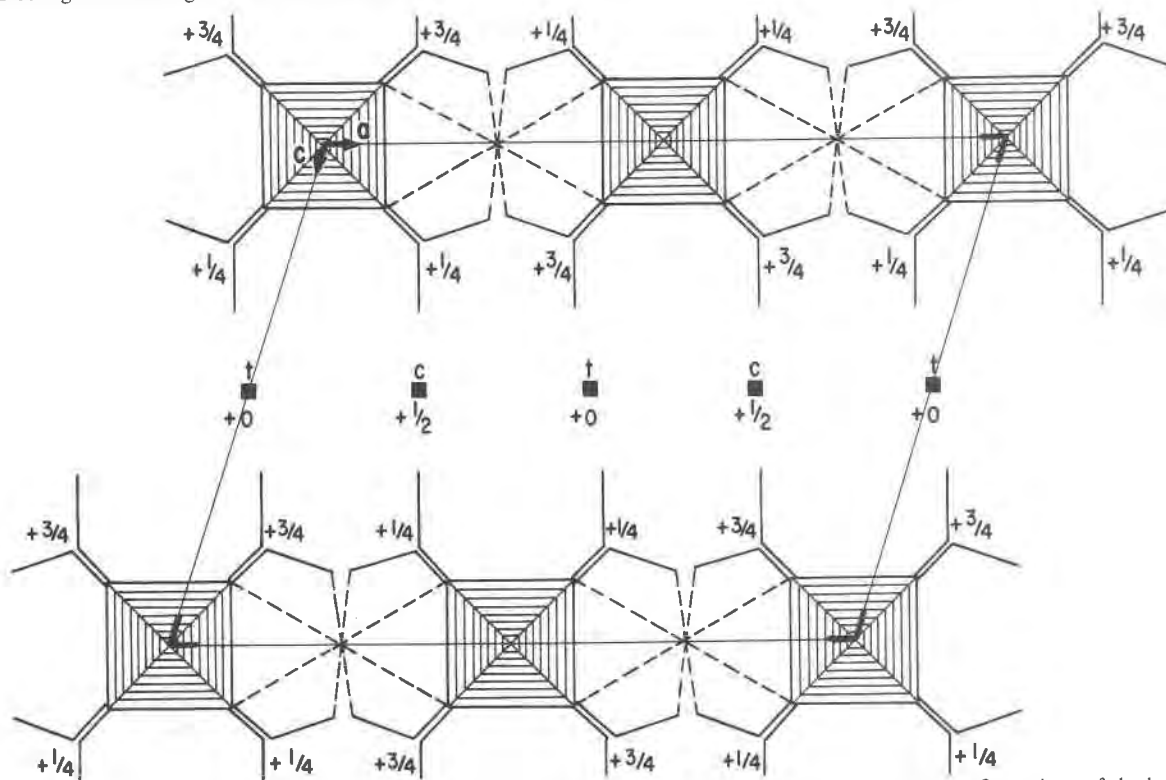

Fig. 4b. Idealized structure of jahnsite fully assembled. Note the alternate *trans*- ("t") and cis- ("c") configurations of the bridging octahedra.
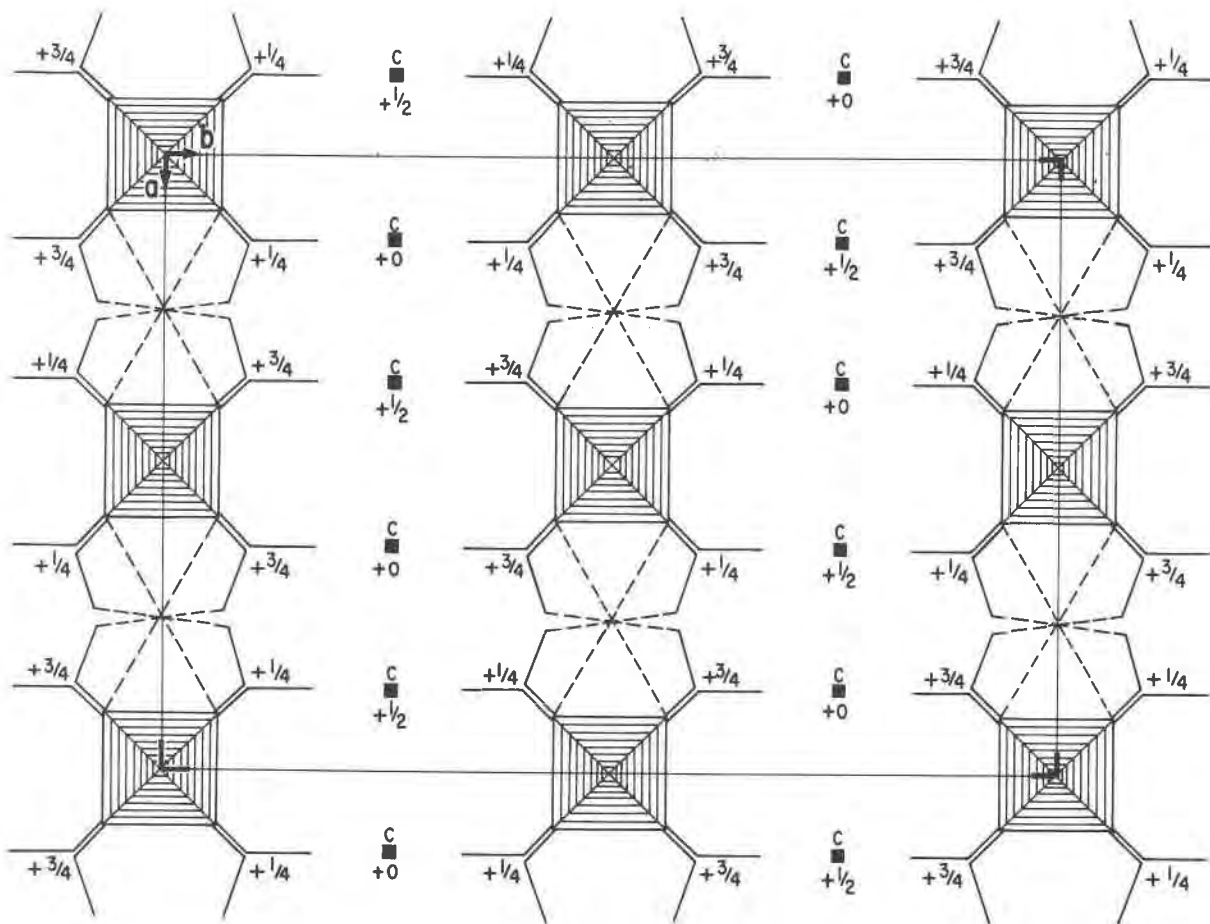
Fig. 4c. Idealized structure of a hypothetical arrangement fully assembled. The space group is *Pbma*. Note the *cis*-configuration for bridging octahedra.

electrostatic repulsion, is not acceptable. In Figure 5, the bond distances and angles are provided and the labelling scheme conforms with the list of polyhedral bond distances in Table 3.

The bonds to anions are tabulated in Table 5, following assignments proposed by Baur (1970). The deviations from local electrostatic neutrality, Δp_x, are then compared with deviations, Δd, in individual bonds from polyhedral averages. Contradictions in bond-length deviations in excess of 0.01A are underlined. Of the eight contradictions, six of them are balanced by positive correlations in the same row. The two remaining contradictions involve OH^-. Moore and Araki (1974) noted that the $Fe^{3+}-OH^-$

distances are also longer than average in the jahnsite structure.

In overite, Ca^{2+} exhibits $6 + 2$ coordination with respect to oxygen. The six inner bonds range from $Ca-O = 2.33$ to 2.49A, and the remaining two outer bonds from 2.79 to 2.86A. The $O-Ca-O$ bond angles are highly distorted for an octahedron, and range from $O(5)^{(5)}-Ca-O(7)^{(5)} = 60.5(1)°$ to $O(5)^{(5)}-Ca-O(7) = 108.5(1)°$. In this study, Ca^{2+} is assumed to be six-coordinated by oxygens. The polyhedral averages are $^{(6)}Al-O = 1.91$, $^{(4)}P(1)-O = 1.54$, $^{(4)}P(2)-O = 1.54$, $^{(6)}Ca-O = 2.40$, and $^{(6)}Mg-O = 2.08A$, in agreement with averages found in related structures.
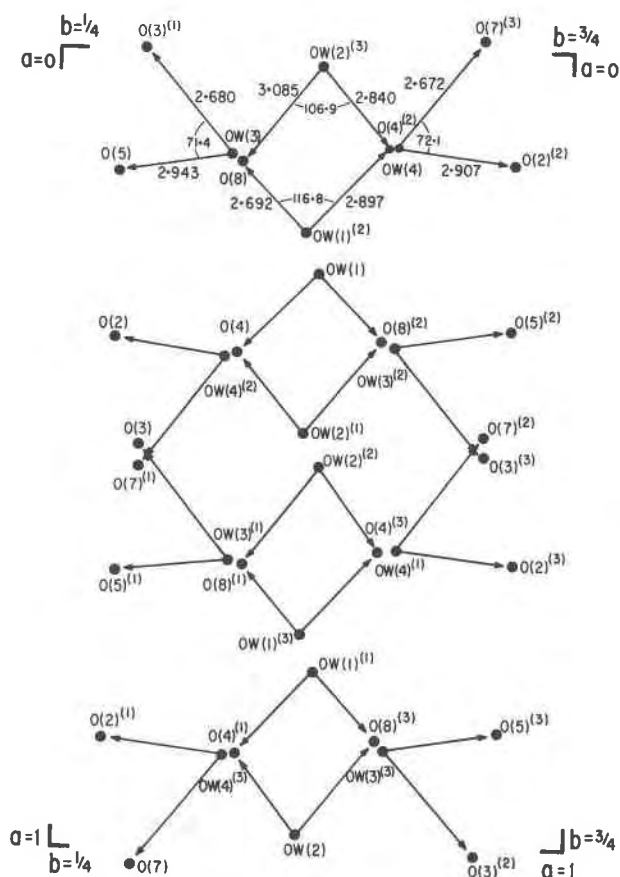
Fig. 5. Hydrogen bonding scheme found in the crystal structures of overite and segelerite. The bond distances refer to those computed for overite. Note the herringbone pattern of bonds which cut the [010] direction. The labelling scheme conforms to Table 3.

For segelerite, the estimated standard deviations in bond distances are up to ±0.01A in Me–O and ±0.02A in O–O', but comparison of distances about the Mg^{2+} cations with those of overite show greatest differences of 0.09A in Mg–O(4)$^{(2)}$ and 0.14A in O(4)$^{(2)}$–OW(1). These distances should not vary substantially in the two structures, since the environments and the kinds of ions are about the same in both. Therefore, it is likely that the inferior quality of the segelerite structure factors affords errors in distances greater than those estimated from the refined coordinate parameters, since correlations in those parameters are high owing to a pronounced substructure.

Acknowledgments

References

Baur, W. H. (1970) Bond length variation and distorted coordination polyhedra in inorganic crystals. *Trans. Am. Crystallogr. Assoc.*, 6, 129–155.

Busing, W. R., K. O. Martin and H. A. Levy (1962) ORFLS, a Fortran crystallographic least-squares program. *U.S. Natl. Tech. Inf. Serv., ORNL-TM-305.*

Cromer, D. T. and D. Liberman (1970) Relativistic calculation of anomalous scattering factors for X-rays. Los Alamos Scientific Laboratory, *Univ. of Calif. Report LA-4403, UC-34.*

—— and J. B. Mann (1968). X-ray scattering factors computed from numerical Hartree-Fock wave-factions. *Acta Crystallogr., A24*, 321–324.

Table 5. Deviations in electrostatic valence bond sums (Δp_x) of cations to anions from neutrality for overite†

	Ca	Mg	Al	P	H_d	H_a	Δp_x	Δd			
								Ca	Mg	Al	P
O(1)			1	1			−0.25			−0.01	−0.01
O(2)	1		1	1		1	+0.25	+0.09		−0.03	+0.01
O(3)	2			1	1	1	+0.08	−0.02,−0.06			+0.01
O(4)		1		1	1	2	−0.08		+0.00		−0.02
O(5)	1		1	1		1	+0.25	+0.07		−0.02	+0.01
O(6)			1	1			−0.25			+0.01	−0.01
O(7)	2			1		1	+0.08	−0.07,−0.02			+0.02
O(8)		1		1		2	−0.08		−0.01		−0.03
OH		2			1		−0.17			+0.02,+0.03	
OW(1)	1				2		+0.00		−0.01		
OW(2)	1				2		+0.00		+0.00		
OW(3)	1				2		+0.00		+0.01		
OW(4)	1				2		+0.00		+0.01		

†The number of bonds each anion receives from cations is listed. Deviations, Δd, in individual bond distances from polyhedral averages are also listed. If Δd contradicts Δp_x, it is italicized.

Larsen, E. S., III (1940) Overite and montgomeryite: two new minerals from Fairfield, Utah. *Am. Mineral., 25,* 315–326.

Moore, P. B. (1970) Structural hierarchies among minerals containing octahedrally coordinating oxygens: I. Stereoisomerism among corner-sharing octahedral and tetrahedral chains. *Neues Jahrb. Mineral. Monatsh., 1970,* 163–173.

—— (1974). I. Jahnsite, segelerite and robertsite, three new transition metal phosphate species. *Am. Mineral., 59,* 48–59.

—— (1975) Laueite, pseudolaueite, stewartite and metavauxite: a study in combinatorial polymorphism. *Neues Jahrb. Mineral. Abh., 123,* 148–159.

—— and T. Araki (1974) Jahnsite, $CaMn^{2+}Mg_2(H_2O)_8Fe_2^{3+}(OH)_2[PO_4]_4$: a novel stereoisomerism of ligands about octahedral corner-chains. *Am. Mineral., 59,* 964–973.

Ramachandran, G. N. and R. Srinivasan (1970) *Fourier Methods in Crystallography.* p. 96–119. Wiley-Interscience, New York.

Zachariasen, W. H. (1968) Experimental tests of the general formula for the integrated intensity of a real crystal. *Acta Crystallogr., A24,* 212–214.